References

1. Fagerstam, L. G.; Pettersson, L. G. *FEBS Lett.* 1979, *98*, 363.
2. Kim, D. W.; Yang, J. H.; Jeong, Y. K. *J. Korean Inst. Chem. Eng.* 1986, *24*, 407.
3. Stahlberg, T.; Johansson, G.; Pettersson, G. *Eur. J. Biochem.* 1988, *173*, 179.
4. van Tilbeurgh, H.; Loontiens, F. G.; Engelborgs Y.; Claeyssens, M. *Eur. J. Biochem.* 1989, *184*, 553.
5. Kim, D. W.; Jeong, Y. K.; Jang, Y. H.; Lee, J. K. *J. Ferment. Bioeng.* 1994, *77*, 363.
6. Bisaria, V. S.; Ghose, T. K. *Enzyme Microb. Technol.* 1981, *3*, 90.
7. Henrissat, B.; Driguez, H.; Viet, C.; Schulein, M. *Bio/Technology* 1990, *3*, 722.
8. Converse, A. O.; Optekar, J. D. *Biotechnol. Bioeng.* 1993, *42*, 145.
9. Schmuck, M.; Pilz, I. *Biotechnol. Lett.* 1986, *8*, 397.
10. Abuja, P. M.; Pilz, I.; Claeyssens, M.; Tomme, P. *Biochem. Biophys. Res. Commun.* 1988, *156*, 180.
11. Abuja, P. M. ; Pilz, I.; Tomme, P.; Claeyssens, M. *Biochem. Biophys. Res. Commun.* 1989, *165*, 615.
12. Stahlberg, J.; Johansson, G.; Pettersson, G. *Bio/Technology* 1991, *9*, 286.
13. Din, N.; Gilkes, N. R.; Tekant, B.; Miller, R. C.; Warren, Jr. R. A. J. *Bio/Technology* 1991, *9*, 1096.
14. Woodward, J.; Affholter, K. A.; Noles, K. K. *Enzyme Microb. Technol.* 1992, *14*, 625.
15. Park, J. S.; Nakamura, A.; Horinouchi, S.; Beppu, T. *Biosci. Biotech. Biochem.* 1993, *57*, 260.
16. Ong, E.; Gilkes, N. R.; Miller, R. C.; Warren, Jr. R. A. J.; Kilburn, D. G. *Biotechnol. Bioeng.* 1993, *42*, 409.
17. Klyosov, A. A. *Biochemistry* 1986, *25*, 540.
18. Klyosov, A. A. *Biochemistry* 1990, *29*, 10577.
19. Lowry, O. H.; Rosebrough, N. R.; Farr, A. E.; Randall, R. J. *J. Biol. Chem.* 1951, *193*, 265.
20. Summer, J. B.; Somers, G. F. In *Laboratory Experimentals in Biological Chemistry*; Academic Press: 1944; p 34.
21. Ooshima, H.; Sakata, M.; Harano, Y. *Biotechnol. Bioeng.* 1983, *25*, 3103.
22. Kim, D. W.; Yang, J. H.; Jeong, Y. K. *Appl. Microbiol. Biotechnol.* 1988, *28*, 148.
23. Lee, S. B.; Shin, H. S.; Ryu, D. D. Y. *Biotechnol. Bioeng.* 1982, *24*, 2137.
24. Steiner, W.; Sattler, W.; Esterbauer, H. *Biotechnol. Bioeng.* 1988, *31*, 853.
25. Tanaka, M.; Ikesaka, M.; Matsuno, R.; Converse, A. O. *Biotechnol. Bioeng.* 1988, *32*, 698.
26. Kim, D. W.; Kim, T. S.; Jeong, Y. K.; Lee, J. K. *J. Ferment. Bioeng.* 1992, *73*, 461.
27. Kim, D. W.; Jeong, Y. K.; Lee, J. K. *Enzyme Microb. Technol.* 1994, *16*, 649.

Monte Carlo Studies of Argon Adsorbed in 5A Zeolite Cavities

Soong-Hyuck Suh*, **Woo-Chul Kim**, **Ki-Ryong Ha**,
Soon-Chul Kim†, Nam-Ho Heo‡, and Keith E. Gubbins#

Department of Chemical Engineering, Keimyung University, Taegu 704-701, Korea
†Department of Physics, Andong National University, Andong 760-749, Korea
‡Department of Industrial Chemistry, Kyungpook National University, Taegu 702-701, Korea
#School of Chemical Engineering, Cornell University, Ithaca, New York 14853, U.S.A.

The grand canonical ensemble Monte Carlo simulations have been carried out to investigate the thermodynamic and energetic properties for the Lennard-Jones system of argon gases adsorbed in 5A zeolites. The adsorption isotherm, the isosteric heat of adsorption and the energy distribution curves are computed at the fixed temperature of 233 K over the bulk pressure range varying from 50 kPa to 400 kPa, and the resulting simulation data are compared with the available experimental values. For temperature and pressure conditions employed in this work the Monte Carlo results are shown to be in reasonable agreement with the corresponding experimental data. Two main peaks in the energy distribution curves are observed due to the energetically distinct regions near the sorption sites of such zeolite cavities.

Introduction

Because of their unique structure with exceptional porosity, zeolite materials have played an important role in industrial applications such areas as purification, separation, catalysis and ion-exchange. In many cases the zeolite struc-

ture remains the fundamental factor responsible for these applications.[1] The pore size, shape and dimensionality of zeolites are dependent not only on the framework cavities but also on the type of neutralizing cations contained in the nonframework structure. For instance, by exchanging the sodium cations in the A-type zeolite with the calcium cations, the

effective aperture diameter is increased from about 4 Å (4A zeolite) to about 5 Å (5A zeolite) while the potassium cations reduce to about 3 Å (3A zeolite). This ion-exchange process may take place readily in an appropriate solution or molten salt.

In order to facilitate the selection and optimization techniques required in the zeolite chemistry, it is frequently desirable to investigate the related thermophysical properties at a molecular level. An alternative approach to this goal is the use of the molecular-based computer simulations[2] *via* Monte Carlo and molecular dynamics methods. In principle, if one has an accurate knowledge of the pore structure and the interaction potentials, then it should be possible to obtain any macroscopic values from this microscopic information. Current computational studies in various zeolite systems can be classified into two groups : those dealing with the idealized pore model as a reference system[3] and those dealing with the more realistic model including complicated geometric factors.[4]

In the present work, we investigate the thermodynamic and energetic properties of argon gases trapped inside 5A zeolite cavities under equilibrium conditions with the external gas phase. To this end, grand canonical ensemble Monte Carlo (GCEMC) simulations have been carried out to elucidate the most important features governing the adsorption characteristics and the related energy distribution within zeolite systems. In the grand canonical ensemble the chemical potential, volume and temperature of the system are fixed, and the equilibrium condition is maintained by requiring that the chemical potential in the adsorbed phase should be equal to that in the bulk phase. Since the number of adsorbed molecules in the pore phase is allowed to fluctuate in this ensemble itself, the GCEMC calculation is most appropriate for determining the adsorption characteristics of model systems distributed between the bulk phase and the pore phase.[5]

Model and Computational Methods

The two-dimensional crystal structure for the unit cell of dehydrated 5A zeolite (the chemical composition, Ca_4Na_4 [$(SiO_2)_{12}(AlO_2)_{12}$]) is illustrated in Figure 1. In this figure the silicon/aluminium/oxygen framework atoms are displayed as ball-and-stick representations. Also shown as the smaller and larger spheres, which are not parts of the zeolite framework but located near the middle of the six-membered oxygen ring, indicate Na and Ca cations in the specific sites, respectively. The atomic coordinates for the crystal structure were taken from the refined atomic positions by the X-ray crystallographic analysis.[6] For computational simplicity, we modelled the rigid zeolite system, in which the positions of both the framework atoms and the cation atoms are fixed. In this model, as a first approximation, the zeolite structure did not alter with the loading of adsorbate molecules during the sorption simulations.

We consider here the case of argon gases adsorbed within the 5A zeolite pores. The interaction energies for argon-argon and argon-zeolite atoms are atomistically calculated using the simple potential function of a pairwise Lennard-Jones 6-12 model. The argon-zeolite interaction parameters appeared in the Lennard-Jones model may be calculated
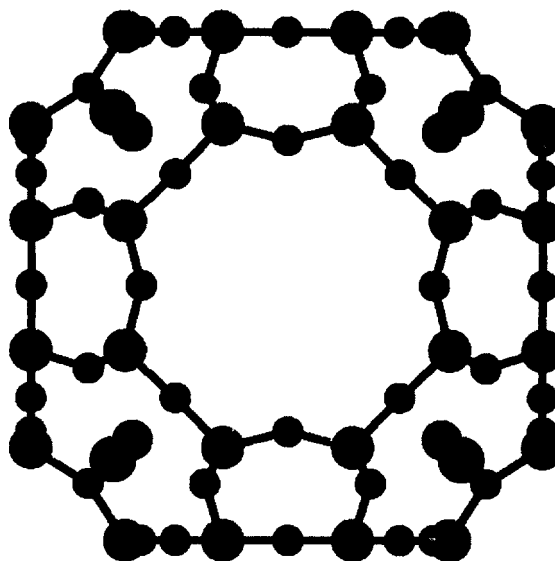

Figure 1. The two-dimensional crystal structure for the unit cell of 5A zeolite with the zeolite framework as ball-and-stick representations. The smaller and larger spheres near the six-membered oxygen ring indicate Na^+ and Ca^{+2} cations, respectively.

using several theoretical predictions, namely, the London equation, the Slater-Kirkwood equation and the Kirkwood-Muller equation. According to Razmus and Hall,[4c] those predictions can give only an estimate of model parameters and the theoretical calculations yield the dispersion constants which differ by as much as a factor of six. The Lennard-Jones potential parameters employed here are chosen to be the same as described elsewhere,[4c],7 in which the empirical method were used to fit the dispersion constant and the corresponding repulsion parameter was derived from the condition that the force must be zero at equilibrium distance. In practice the choice of a particular model potential and the level of approximation depend directly on simulation qualities that one is specifically interested in. Any choice involves a compromise between the quality of simulations and the amount of computing time. The possible induced effects due to the electric fields are ignored in modelling the argon-zeolite potentials since the polarizability of argon is known to be sufficiently small. In fact the long-ranged charge distributions in many silicalite materials are largely delocalized.[4f] Consequently, the electrostatic interactions can be neglected for the small and nonpolar molecules confined within zeolites. It should be pointed out, however, that such an assumption used in our case of argon sorbates may not be valid for larger and more polarizable molecules, for example, chain molecules.[4d]

The problem of describing an analytical model potential for the zeolite system is not trivial. The charged cations and the oxygen atoms distributed in the zeolite framework retain a certain amount of ionic character, which in principle cannot be neglected. Our approach arises from the need for a simple 'effective' model that is able to reproduce the equilibrium features of rare gases adsorbed in zeolite cavities. Such a Lennard-Jones potential was successfully employed in the previous simulation studies of rare gases adsorbed in zeolite
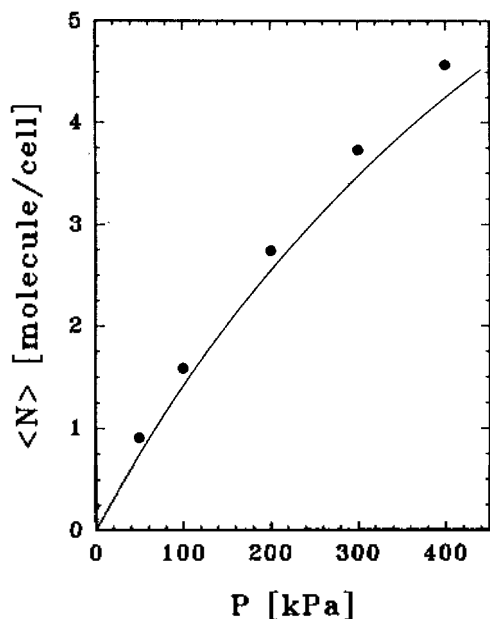
Monte Carlo Studies of Argon Adsorbed in 5A Zeolite Cavities

Bull. Korean Chem. Soc. 1995, Vol. 16, No. 8   727

Figure 2. Adsorption isotherm as a function of bulk pressure. ● GCEMC results; — experimental data.[10]
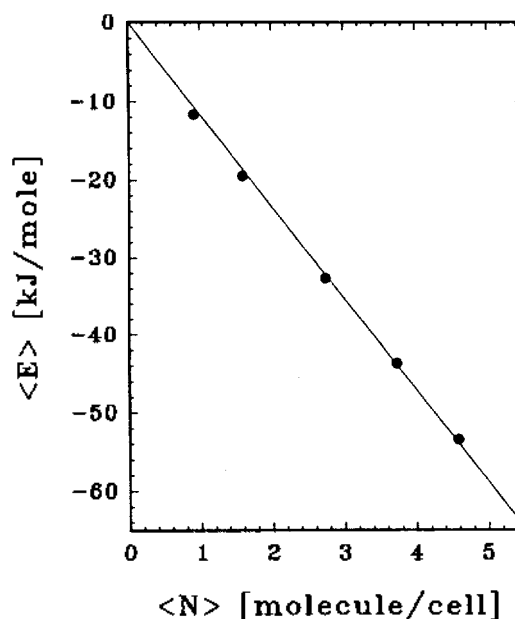

Figure 3. Total potential energy as a function of the amount adsorbed in the unit cell. ● GCEMC results; — the least-square curve fitting.

cavities, for example, argon in 4A zeolite,[4c] and xenon in zeolite X and Y[4b] and in NaA zeolite.[4b] Some applications[1,2] would require more refined molecular degrees of freedom and more sophisticated potentials including the electrostatic interactions and the surface-mediated indirect interactions.

The GCEMC simulations adopted here are based on the asymmetric sampling algorithm proposed by Adams.[8] The main loop consists of two independent steps. In the first step, a particle is randomly moved within a given maximum displacement. The move is either accepted or rejected subject to the total potential energy change. This procedure is exactly the same as the conventional canonical ensemble Monte Carlo method. The second step generates new trial configurations by attempting an addition or removal of a randomly chosen particle. The success of either an addition or removal is controlled both by the potential energy change and by the chemical potential parameter. This compound event is repeated as many times as is desired and the equilibrium properties are evaluated at each step. A more detailed computational method is presented in our previous studies[9] for the hard-sphere and Lennard-Jones systems confined within various porous media.

The initialization procedure was first to construct the computer-generated zeolite structure, and then proceeded directly to the sorption simulations in the accessible pore volume. In order to minimize the system size effects the nearest image convention via periodic boundary conditions was applied in the fundamental cubic box consisting of the 2×2×2 unit cells (384 oxygens, 96 silicons, 96 aluminiums and 64 cations). A spherical cut-off distance was taken as half the simulation box length. During the initial stages of a simulation the configurations generated were not representative of the equilibrium ensembles and were discarded from the averaging process. In all cases reported here configurations were equilibrated for 1×10^5 steps before accumulating data

and the resulting ensemble averages were obtained during the final 2 million simulation steps.

Results and Discussion

The GCEMC simulations were performed at the fixed temperature of 233 K over the bulk pressure range varying from 50 kPa to 400 kPa. In Figure 2 the adsorption isotherm, constructed from the ensemble averages of the number of adsorbed molecules per unit cell, is presented as a function of bulk pressure. The value of bulk pressure in the gas phase is calculated from the corresponding chemical potential with the assumption that the ideal gas law applied. Also shown in this figure as a solid curve are the experimental data measured by Miller *et al.*[10] These experimental data were reported in terms of the modified Langmuir equation with correlation parameters given in this work. The simulation results for the adsorption isotherm are shown to be in good agreement with the available experimental isotherm. This indicates that the atomic-type potentials based on a Lennard-Jones model is, at least qualitatively, of reasonably accuracy to predict such thermodynamic properties for temperature and pressure conditions considered here.

The initial increase in the adsorption isotherm results primarily from the attractive interactions due to the argon-zeolite potentials. At the limit of very low surface coverage, known as the Henry's law regime, the adsorbate-adsorbent energies dominate the adsorbate-adsorbate energies. For higher bulk pressure or higher surface coverage, the cavity-filling effects are increased due to the increasing importance of the repulsive interactions among sorbate molecules. Under these conditions the larger deviation from Henry's law at higher coverage is caused by the thermal energy balance between the argon-argon and the argon-zeolite interactions.
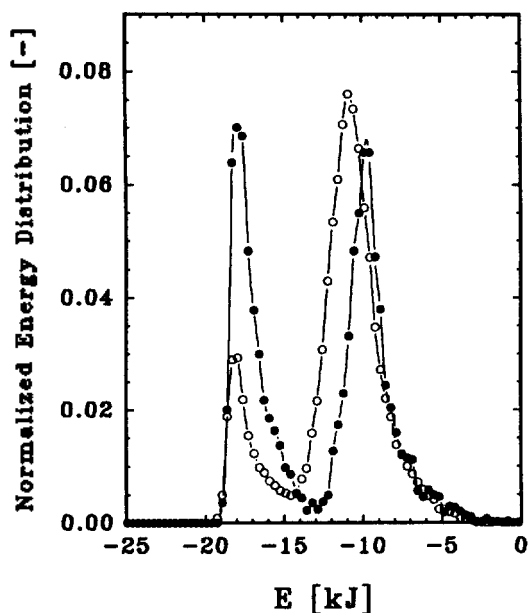
728 *Bull. Korean Chem. Soc.* **1995**, Vol. 16, No. 8

Soong-Hyuck Suh et al.

Figure 4. Normalized energy distributions for different bulk pressures. ● 50 kPa; ○ 400 kPa.

This explains in part that the results of sorption simulations are gradually overestimated with increasing bulk pressures. It can be expected, if this were our case, that the much greater influence among sorbate molecules will be exerted than might be inferred from the simple Lennard-Jones interactions.

The experimental value for the isosteric heat of adsorption was measured to be 14.02 kJ/mol for the system of argon in 5A zeolites.[10] This agrees well with our GCEMC simulation results of 13.84 kJ/mol, which was determined from the slope of the total potential energy versus the amount adsorbed in the unit cell (Figure 3). The good agreement between simulation and experiment again confirms the quality and accuracy of our GCEMC calculation. As can be seen in this figure, the isosteric heat of adsorption obtained here is nearly independent of the coverage, suggesting that the gas adsorption in this range of bulk pressures occurs on the sterically homogeneous surface.

In Figure 4 the normalized energy distribution curves for 50 kPa and 400 kPa are plotted to illustrate the manner in which the energy distributions change with increasing bulk pressure. The distribution energies are clearly found to be the two-peaked curves in shape. The resulting distribution curves correspond to the energetically distinct regions in the zeolite cavities. The energy peak around -18 kJ arise from argon trapped near the localized adsorption sites, whereas the peak in the higher energies around -10 kJ$\sim$ -12 kJ from those located in the less favored regions. These two main peaks are essentially associated with the different adsorption positions, and, obviously, the latter is more mobile because it is occupying the higher energy sites. This indicates that the interaction energy of adsorbed molecules is a strong function of the adsorption site in the zeolite pore phase. As we increase bulk pressures, the actual pore configurations change from the monolayer structure against the zeolite pore wall to the promotion of the second layer forma-

tion. As a consequence of the three-dimensional symmetry in the unit cell of 5A zeolites, there are the eight equivalent sites near cations located in the framework cavities.

A similar trend was observed in the more complex systems studied by Woods and Rowlinson.[4b] In this simulation work they attempted to understand the structural behavior of xenon and methane adsorbed in the systems of zeolite X and also zeolite Y. The molecular structure of methane is nearly spherical in shape and the hard-sphere diameter of methane is roughly equal to that of xenon. The resulting density profiles for methane were qualitatively the same as those for xenon. At the low pressure region sorbate molecules formed a predominantly monolayer structure in contact with the cavity wall. With increasing pressure there was a second layer near the cavity center and a distance between two layers was found to be approximately equal to the equilibrium molecular separation. The experimental measurements of xenon[11a] and methane[11b] in the systems of zeolite A found that adsorbed molecules were bound close to the cavity wall with the promoted layer corresponding to the potential minima. Although the exact comparison with our GCEMC results is not expected, the structural effects explained in this work are in agreement with those computational and experimental observations.

In summary, we have demonstrated that the microscopic behavior of adsorption characteristics would be very sensitive to the underlying molecular-scale event. Our GCEMC computations, coupled with the Lennard-Jones 12-6 model as an input potential, qualitatively reproduce the equilibrium and thermodynamic properties such as the adsorption isotherm and the isosteric heat of adsorption that are in close agreement with the available experimental data. Molecular-based computational approaches can also provide the detailed information about the related energetic properties at a molecular level. Although we have restricted our attention to the case of argon in 5A zeolites using the relatively simple model potentials, it would be of great interest to investigate other zeolite systems in order to verify a number of the conclusions observed here, which may be difficult to probe by the experimental measurement. More precisely defined molecular interactions and electrostatic effects would be required for this application. Confirmation of obtaining this possibility is currently under investigation and further simulation results will be reported in the near future.

References

1. Cheetham, A. K.; Gale, J. D. In *Modelling of Structure and Reactivity in Zeolites*; Catlow, C. R. A. Ed.; Academic Press: New York, 1992, p 63.
2. Titiloye, J. O.; Tschaufeser, P.; Parker, S. C. In *Spectroscopic and Computational Studies of Supramolecular Systems*; Davies, J. E. D. Ed.; Kluwer Academic Publishers: Netherlands, 1992, p 137.
3. (a) Soto, J. L.; Myers, A. L. *Mol. Phys.* **1981**, *42*, 971.

(b) Woods, G. B.; Panagiotopoulos, A. Z.; Rowlinson, J. S. *Mol. Phys.* **1988**, *63*, 49. (c) Baksh, M. S. A.; Yang, R. T. *AIChE J.* **1991**, *37*, 923. (d) Cracknell, R. F.; Gordon, P.; Gubbins, K. E. *J. Phys. Chem.* **1993**, *97*, 494. (e) Suh, S.-H.; Park, H.-K. *Korean J. Chem. Eng.* **1994**, *11*, 198.

4. (a) Yashonath, S.; Demontis, P.; Klein, M. L. *Chem. Phys. Lett.* **1988**, *153*, 551. (b) Woods, G. B.; Rowlinson, J. S. *J. Chem. Soc. Faraday Trans. 2* **1989**, *85*, 765. (c) Razmus, D. M.; Hall, C. K. *AIChE J.* **1991**, *37*, 769. (d) Snurr, R. Q.; June, R. L.; Bell, A. T.; Theodorou, D. N. *Mol. Simul.* **1991**, *8*, 73. (e) Santikary, P.; Yashonath, S. *J. Chem. Soc. Faraday Trans.* **1992**, *88*, 1063. (f) Cracknell, R. F.; Gubbins, K. E. *Langmuir* **1993**, *9*, 824. (g) Van Tassel, P. R.; Davis, H. T.; McCormick, A. V. *J. Chem. Phys.* **1993**, *98*, 8919. (h) Jameson, C. J.; Jameson, A. K.; Baello, B. I.; Lim, H.-M. *J. Chem. Phys.* **1994**, *100*, 5965.

5. Nicholson, D.; Parsonage, N. G. In *Computer Simulation and the Statistical Mechanics of Adsorption*; Academic Press: New York, 1982; Chap. 5.

6. Szostak, R. In *Handbook of Molecular Sieves*; Van Nostrand Reinhold: New York, 1992.

7. Lee, L. L. In *Molecular Thermodynamics of Nonideal Fluids*; Butterworth Publishers: London, 1988; Chap 9.

8. (a) Adams, D. J. *Mol. Phys.* **1974**, *28*, 1241. (b) *ibid.* **1975**, *29*, 307.

9. (a) MacElroy, J. M. D.; Suh, S.-H. *AIChE Symp. Ser.* **1986**, *82*, 133. (b) MacElroy, J. M. D.; Suh, S.-H. *Mol. Phys.* **1987**, *60*, 475. (c) MacElroy, J. M. D.; Suh, S.-H. *Mol. Simul.* **1989**, *2*, 313. (d) Suh, S.-H.; Kim, J.-S.; Park, C.-Y. *Hwahak Konghak* **1991**, *29*, 742.

10. Miller, G. W.; Knaebel, K. S.; Ikels, K. G. *AIChE J.* **1987**, *33*, 194.

11. (a) McCormick, A. V.; Chmelka, B. F. *Mol. Phys.* **1991**, *73*, 603. (b) Cohen de Lara, E.; Seloudoux, R. *J. Chem. Soc. Faraday Trans. 1* **1983**, *79*, 2271.

A Theoretical Investigation of the CO Adsorption on Cobalt Surfaces: Co(0001), (10T0), (11Z0), and (10T2)

Yon-Tae Je* and Audrey L. Companion

*Department of Chemistry, Gyeongsang National University, Chinju 660-701, Korea
Department of Chemistry, University of Kentucky, Lexington, KY 40506, U.S.A.

Binding characteristics of single CO molecules adsorbed on cobalt surfaces: Co(0001), (10T0), (11Z0), and (10T2) were investigated theoretically employing the semi-empirical ASED-MO method to help better understand the mechanism of CO dissociation on these cobalt surfaces. On all these surfaces, there were observed gradual increases in optimum C-O and Co-C distances (dC-O and dCo-C) and the consequent decreases in C-O and Co-C bond orders (pC-O and pCo-C), and small increases in binding energy (BE) and relative stability of CO to the surface as the binding site of CO changes from on-top to 2-fold bridge and/or to 3-fold bridge (or hollow) site on a given specific layer, the same trend in most calculation works. For such site change of CO, stretching C-O vibrational frequencies (vC-O) decreased significantly on all cobalt crystal surfaces and the corresponding cobalt-C stretching frequencies (vCo-C) also dropped, but not as strongly as the vC-O. For example, from a CO on the (0001), vC-O decreases from 1969-1992 cm-1 for on-top to 1693-1763 cm^{-1} for 2-fold bridge and then to 1560-1635 cm^{-1} for 3-fold hollow site CO species and their >vCo-C declines from 569-590 cm^{-1} to 472-508 cm^{-1} and then to 470-482 cm^{-1}. In addition, atomic C-Co stretching frequencies were computed as a possible aid in a future experiment.

Introduction

Transition metals have been paid a significant amount of attention through several decades as catalysts for hydrocarbon synthesis reactions such as the Fischer-Tropsch reaction; the catalytic conversion of synthesis gas (CO and H_2) to chain hydrocarbons.[1,2] It was widely admitted that the first step in Fischer-Tropsch processes is the dissociation of CO molecules on a metal surface to form mainly surface carbidic (rather than graphitic) carbon and oxygen, then followed by the hydrogenation of carbidic carbon to form hydrocarbons.[3,4] In order to help better understand the mechanism of this CO dissociation on metal surfaces, there have been numer-

ous studies on the surface structure and binding sites of carbon monoxide on surfaces of several transition metals such as nickel, iron, platinum, and ruthenium.

Here are abstracted some distinguished experimental and theoretical achievements from those studies. The interaction between CO and metal surface has been portrayed traditionally by the Blyholder model,[5] in which bonding in a metal-carbonyl complex is depicted by the CO 5σ to metal forward donation and metal d to CO $2\pi^*$ back-donation, with some support[6] and criticism[7] later. Several experimental and theoretical studies indicated that CO adsorbs (or binds) in the end-on orientation with the carbon-end toward a metal surface for transition metals in the right-side of the periodic